A ROBUST MODEL PREDICTIVE CONTROL FOR EFFICIENT THERMAL MANAGEMENT OF INTERNAL COMBUSTION ENGINES

Francesco Pizzonia[1], Teresa Castiglione[1] and Sergio Bova[1,*]

[1]DIMEG, Department of Mechanical, Energy and Management Engineering,
Università della Calabria, Via P. Bucci, Cubo 44C, 87036 Rende, ITALY

[*]Corresponding author: tel. +39 0984 494828, email address: sergio.bova@unical.it

ABSTRACT

Optimal thermal management of modern internal combustion engines (ICE) is one of the key factors for reducing fuel consumption and CO_2 emissions. These are measured by using standardized driving cycles, like the New European Driving Cycle (NEDC), during which the engine does not reach thermal steady state; engine efficiency and emissions are therefore penalized. Several techniques for improving ICE thermal efficiency were proposed, which range from the use of empirical look-up tables to pulsed pump operation. A systematic approach to the problem is however still missing and this paper aims to bridge this gap.

The paper proposes a Robust Model Predictive Control of the coolant flow rate, which makes use of a zero-dimensional model of the cooling system of an ICE. The control methodology incorporates explicitly the model uncertainties and achieves the synthesis of a state-feedback control law that minimizes the "worst case" objective function while taking into account the system constraints, as proposed by Kothare et al. in 1996. The proposed control strategy is to adjust the coolant flow rate by means of an electric pump, in order to bring the cooling system to operate around the onset of nucleate boiling: across it during warm-up and above it (nucleate or saturated boiling) under fully warmed conditions. The computationally heavy optimization is carried out off-line, while during the operation of the engine the control parameters are simply

picked-up on-line from look-up tables. Owing to the little computational effort required, the resulting control strategy is suitable for implementation in the ECU of a modern engine.

The control strategy was validated by means of experimental tests under several operating conditions, involving both warm-up and fully warmed engine thermal states. The tests were carried out with a small displacement Spark-Ignition Engine which was equipped with an electric coolant pump, directly driven by the control algorithm.

Results show that the controller is robust in terms of disturbance rejections, it respects the defined system constraints and is also very fast in terms of response to the perturbations. The experimental tests proved that the proposed control is effective in decreasing the warm-up time and in reducing the coolant flow rate under fully warmed conditions as compared to a standard configuration with pump speed proportional to engine speed. The adoption of these cooling control strategies will, therefore, result in lower fuel consumption and reduced CO_2 emissions.

HIGHLIGHTS

- A Robust Model Predictive Control for ICE Thermal Management was developed.
- The proposed control is effective in decreasing the warm-up time.
- The control system reduces coolant flow rate under fully warmed conditions.
- The control strategy operates the cooling system around onset of nucleate boiling.
- Little on-line computational effort is required.

KEYWORDS

Thermal Management; CO_2 reduction; Nucleate Boiling; Cold Start; Robust Control; Model Predictive Control; Internal Combustion Engines.

NOMENCLATURE

A	engine surface area[m^2]
A_{nb}	part of engine surface involved in nucleate boiling [m^2]
bmep	engine brake mean effective pressure (bar)
c	constant value in Eq.3.

c_p	coolant specific heat [J/kg K]
C_c	coolant thermal capacity [kJ/K]
C_w	engine thermal capacity [kJ/K]
h_{mac}	macro-convection heat transfer coefficient [W/m^2 K]
h_{mic}	micro-convection heat transfer coefficient [W/m^2 K]
K_1, K_2	values of the controller
$\dot{m}_c$	coolant flow rate [kg/s]
$\dot{m}_f$	fuel flow rate [kg/s]
N	engine speed in Eq.3[rpm]
n	exponent in Eq.3
n_1	exponent in Eq.3
n_2	exponent in Eq.3
p	coolant pressure [bar]
q_{ONB}	nucleate boiling heat flux [W/m^2]
q_w	combustion chamber thermal flux [W/m^2]
$\dot{Q}_c$	thermal power removed by the coolant from the combustion chamber walls[W]
$\dot{Q}_g$	thermal power supplied by the fuel to the combustion chamber walls [W]
$\dot{Q}_r$	thermal power supplied by the coolant to the radiator [W]
T_c	coolant temperature [K]
T_{c_eq}	equilibrium coolant temperature [K]
T_{in}	coolant temperature at engine inlet [K]
T_{ONB}	wall temperature for onset of nucleate boiling [K]
T_{out}	coolant temperature at engine outlet [K]
T_{sat}	saturation temperature[K]
T_w	engine wall temperature [K]
T_{w_eq}	equilibrium engine wall temperature [K]
T_∞	bulk flow temperature [K]

1. INTRODUCTION

A wide variety of innovative technologies are under development for meeting the requirements of regulatory agencies on vehicle emissions [1,2]. Most of them point towards an increase in engine efficiency and fuel saving and many are already on the market. An optimal engine thermal management constitutes one of the most promising solutions and can be achieved at very limited costs, with respect to the various technological options. Cipollone and Battista [3] show that the cooling system management offers interesting possibility for efficiency increase at the very limited cost of about 200 €/km/l of saved fuel. A comprehensive review of influences of thermal management on internal combustion engines efficiency was also reported by Roberts et al. [4]. The main effort aims to speed up the warm-up time during a standard homologation cycle, where the major part of pollutant emissions and engine inefficiency happens after the cold start. Engine efficiency and emissions are, in fact, heavily influenced by the thermal conditions; although typical part-load efficiency is about 20-25% for a Spark Ignition engine and about 30% for a diesel engine [5], this efficiency drops to about 9% after a cold start [6,7].

Low engine temperatures determine poor engine efficiency and emissions due to increased friction losses and to combustion inefficiency. The main factor responsible for this is the cylinder liner mid-stroke temperature; this temperature, in fact, influences the lubricant temperature and, therefore, the friction losses, especially during warm-up. Under low lubricant temperature conditions (around 20 °C) Will et al. [6, 8] estimated that frictional losses can be up 2.5 times higher than the ones in fully warmed conditions and Samhaber et al. [9] predicted an increase of about 13.5% in fuel consumption if the temperature is even lower, around 0 °C. In addition, the cylinder liner temperature influences directly the temperature of the unburned gases within the crevices volumes inside the combustion chamber, which are the main source of unburned hydrocarbon emissions in Spark Ignition Engines [10].

Mid-stroke cylinder liner temperature can be controlled by means of the coolant flow rate. During warm-up, when the radiator is by-passed and the coolant temperature at engine-inlet is almost equal to the coolant engine-out one, by diminishing the coolant flow rate, a decrease of coolant temperature and an increase of liner temperature can be achieved [11]. On the other hand, under steady state conditions, by keeping the engine-in coolant temperature constant, both the engine-out coolant temperature and the head and cylinder block temperature increase as coolant flow rate diminishes [12]. As the cooling pump is driven by the crankshaft today, its

speed is proportional to that of the engine, so that the coolant flow rate can only be reduced by using the thermostatic valve. According to Brace [13], as a result of this poor regulation capability, engines are over-cooled for about 95% of their operating time.

Several different techniques were proposed for controlling the coolant flow rate independently of engine speed, all of them focusing on using electrically driven pumps. Ap and Golm [14] first addressed the issue of cost reduction of engine cooling components and proposed the use of a small electric water pump with reduced coolant flow rates. Brace [13] proposed the use of an electric pump in a control strategy, which was based on the use of empirical look-up tables. More recently the same author [15], again using electrically driven pumps, found that a 2% improvement in bsfc was obtained by reducing the coolant flow rate by means of a throttle valve. Bent [16] adopted a pulsed coolant flow strategy with an electric pump switched ON and OFF in order to circulate the coolant only when it was required. Other types of pump could be used for controlling the coolant flow rate, like variable-displacement vane pumps [3, 17], which are currently adopted in the lubricating system of some ICE. Electric pumps are usually preferred in laboratory tests owing to their ease of use.

A more systematic approach to coolant flow rate control can however be adopted, which can make use of the recent developments of the control and optimization techniques. As most of the energy plants are MIMO (Multi Input Multi Output) systems, it is not possible to adopt straightforward classical control approaches with them, such as the PID control. A widely used approach for MIMO slow-dynamical systems is the Model Predictive Control (MPC), where a model of the plant is used to evaluate the system evolution [18,19]. Several researchers used the MPC technique in different fields for increasing energy efficiency. For example, van Staden et al. [20] employed this procedure to optimize the shifting of electricity demand from peak demand periods to off-peak ones; Parisio et al. [21] used the same approach to minimize the operating cost of a micro-grid while satisfying the required energy demand; Kwak et al. [22] adopted this method for analyzing the energy saving in a building. As a general conclusion, Model Predictive Control provides much better results than alternative methods of multi-variable control [19].

The MPC presents, nevertheless, the drawback of excessively heavy on-line computations, while the time for the control actions is strictly limited. The way to avoid this difficulty is indicated by Wan and Kothare [23]: the operating region of the plant is split into small sub-

regions and a set of local predictive controllers are estimated for each of them off-line. The on-line controller then simply switches between the set of local controllers so that the nonlinear transitions from one sub-region to another is fast and smooth, while stability is guaranteed [23].

However, as the models which are used in the MPC technique are only an approximate representation of the physical problem, there is always a certain level of uncertainty in the controlled process. The capability of handling the uncertainty in the mathematical model of a system is widely known as *robustness* and controllers, which perform well in the presence of bounded uncertainty are called *robust* controllers [24]. At the same time, the system to be controlled is also subjected to unpredictable and uncontrollable inputs (disturbances) whereas the control inputs and the controlled outputs must obey given constraints. Therefore, the control synthesis must also incorporate the presence of such disturbances, of noise measurements, and of constraints on input and output values. One of the most efficient solutions to these issues is to formulate the design of such a *robust* MPC as a *min-max* (minimization of the worst case) optimization problem with constraints by using the LMI (Linear Matrix Inequality) [18]. In spite of the wide spread of the above mentioned method, the approach of Model Predictive Control was never proposed to optimize the Thermal Management of Internal Combustion Engines.

In the present paper a novel Robust Model Predictive Control of engine cooling is presented, which is based on the use of an electric pump and on the possibility of predicting the heat transfer regime which takes place in the cooling system for given values of fuel flow rate, coolant pressure and coolant temperature [12]. The proposed strategy takes advantage of the possibility of operating, around nucleate boiling, with significant lower coolant flow rates than usually adopted, for a faster warm-up and also at fully warmed engine. Several experimental campaigns were carried out in order to identify the most appropriate measurable quantity that could monitor the onset of Nucleate Boiling [25, 26]. The conclusion was that, even though it is possible to identify the onset of nucleate boiling in test rig experiments, this is not feasible on board a vehicle [26]. On the contrary, a rather low computational-effort lumped parameter model, which requires simple and usually already available on-board input data [12], proved suitable to identify the cooling flow regime in a reliable way. In order to develop the control algorithm, the fuel flow rate-speed range of the engine operating conditions was split into sub-regions, so that the constraints can be meaningful and the optimization algorithm gives a solution. The synthesized control was then validated at the engine test-rig. The control design

procedure can be applied to a variety of objectives for the cooling system as well as to different future homologation cycles currently under study. In the present work it was applied in order to obtain a fast warm-up and an efficient cooling action with low coolant flow rates under nucleate boiling regime.

The paper is organized in the following way: the model used for predicting the nucleate boiling [12] is briefly summarized and an index (*NB_index*), which measures the distance of the heat transfer regime from the on-set of nucleate boiling, is defined; next, the control strategy, which is based on the previously mentioned model, is exposed and the problem formulation is presented [18]; the procedure for actually implementing the proposed control strategy is then outlined; finally, the experimental tests at the engine test rig are described and the results of the proposed model are presented in terms of both warm up performance and fully warmed behavior.

2. COOLING SYSTEM MODEL

A zero-dimensional model of the cooling system of an ICE was developed by Bova et al. [12], with the aim of predicting dynamically the heat transfer mechanism within the cooling system of internal combustion engines. The model, which was designed to predict both forced convection and nucleate boiling flow regime, calculates the engine average wall temperature, the heat flux at engine walls, the average coolant temperature and the amount of engine wall area involved in nucleate boiling. Other variables of interest can be also computed. The required input data are coolant flow rate, engine-in coolant temperature and pressure, fuel flow rate and engine speed (Fig. 1).

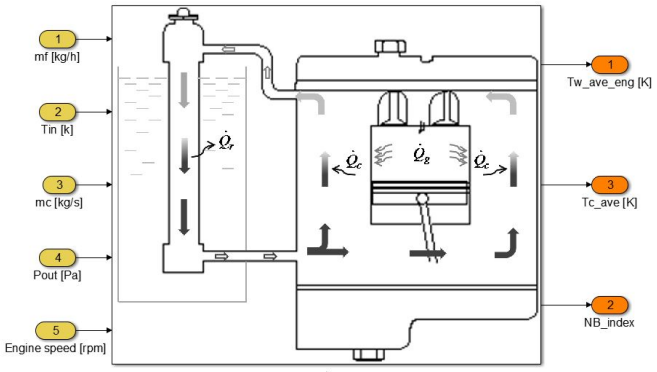

Fig.1 Model input and output variables.

The basic model equations are the ones of energy conservation:

$$\dot{T}_w C_w = \dot{Q}_g - \dot{Q}_c \qquad (1)$$

$$\dot{T}_c C_c = \dot{Q}_c - \dot{Q}_r \qquad (2)$$

which compute the spatial-averaged wall and coolant temperature, T_w and T_c. C_w and C_c are the engine and coolant thermal capacities, respectively; $\dot{Q}_g$, $\dot{Q}_c$ and $\dot{Q}_r$ are the thermal power transferred by the combustion gases to the engine walls, by the engine walls to the coolant and by the coolant to the radiator respectively. For $\dot{Q}_g$ a modified form of the empirical formulation present in [27], which correlates the fuel thermal power to the fuel flow rate, $\dot{m}_f$, to the coolant flow rate, $\dot{m}_c$, and to engine speed, N, was proposed:

$$\dot{Q}_g = c \cdot N^{n_1} \dot{m}_c^{n_2} \dot{m}_f^{n} \qquad (3)$$

where c, n, n_1 and n_2 were estimated through an experimental procedure.

The thermal power transferred to the coolant by the engine walls, $\dot{Q}_c$, is computed through Eq.(4):

$$\dot{Q}_c = h_{mac} A\left(T_w - T_\infty\right) + h_{mic} A_{nb}\left(T_w - T_{sat}\right) \qquad (4)$$

which is composed of two main contributions: the forced convection and nucleate boiling. In Eq. 4, A is the total heat exchange area, while A_{nb} is the part of the engine walls involved in the nucleate boiling phenomenon. Furthermore, h_{mac} and h_{mic} are the heat transfer coefficients owing to forced convection and nucleate boiling respectively; h_{mac} is computed through *Dittus-Boelter* correlation [28], whereas the *Chen* approach is used for heat exchange in nucleate boiling flow regimes (h_{mic}) [29].

The thermal power, released by the coolant to the atmosphere through the radiator, is obtained by the following equation:

$$\dot{Q}_r = \dot{m}_c c_p \left(T_{out} - T_{in}\right) \qquad (5)$$

where T_{in} and T_{out} are the coolant engine-in and engine-out temperatures.

The model computes both the heat flux needed for the onset of nucleate boiling, q_{ONB}, and the corresponding wall temperature, T_{ONB}. The needed heat flux, in particular, is helpful for the definition of the *NB_index*, which will be used in the control algorithm. The *NB_index* is defined as:

$$NB\_index = \frac{\left(q_w - q_{ONB}\right)}{q_{ONB}} \qquad (6)$$

Positive values of the *NB_index* indicate that nucleate boiling occurs, owing to the fact that the actual thermal flux, q_w, is higher than the needed one, q_{ONB}; on the contrary, negative values of the *NB_index* indicate that the actual thermal flux is lower than the needed one and the cooling action is due to forced convection only.

Figure 2 (top) shows the predicted dependence of *NB_index* on the coolant volumetric flow rate for different values of the coolant pressure, 1.3, 1.5, 1.8 bar (lines). The other parameters (engine-inlet coolant temperature, engine rotational speed and fuel mass flow rate) were kept constant. At a given coolant flow rate the *NB_index* increases as the coolant pressure decreases, so that nucleate boiling occurs at about 500 dm^3/h larger coolant flow rate if the coolant pressure decreases from 1.8 to 1.3 bar. The symbols show the *NB_index* variation as calculated by the model on the basis of test-rig data under nominally constant values of engine-inlet coolant temperature, engine rotational speed and fuel mass flow rate. The figure also shows that the thermal power transferred to the coolant steadily diminishes as the coolant flow rate is reduced and that this power is not determined by coolant pressure (Fig. 2 bottom, line); symbols represent experimental data at a coolant pressure of 1.5-1.6 bar. Figure 2 is useful to define a possible control strategy. During warm-up, the smallest possible coolant flow rate should be used, in order to minimize the thermal power transferred to the coolant, while increasing the one transferred to the metal and therefore to the lubricant. This goal must be pursued with respect of the constraints on the coolant and wall temperature values, as well as on a "reasonable" value of the *NB_index*. Also during fully warmed operation, the goal will be the same (the smallest possible coolant flow rate), but the values of the constraints on the temperature and on the *NB_index* will be generally higher and they can take into account requirements on pollutant reduction or knock tendency.

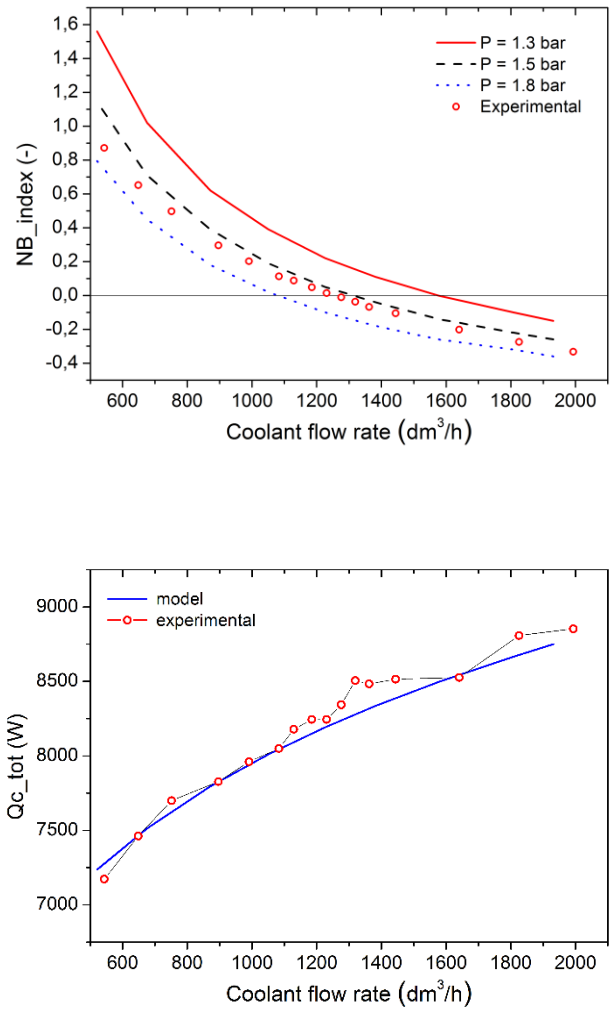

Fig.2 Predicted *NB_index* values for different coolant flow rates (top) and thermal power transferred to the coolant as a function of the volumetric coolant flow rate (bottom). Symbols refer to calculated quantities during test-rig experiments. (Operating conditions: 200 rpm, 2 bar bmep).

3. CONTROL STRATEGY

The goal of the control strategy is twofold: at cold start, a reduction of warm-up time is desirable in order to reduce frictional losses and fuel consumption; this can be achieved with lower values of the coolant flow rate than the ones usually enforced by the belt-driven pump,

which determine heat transfer regime around nucleate boiling. At fully warmed condition, even more intense nucleate boiling flow will be allowed so that the system can work with lower coolant flow rates, while respecting the limits on engine temperature and preserving the engine reliability. The thermal flow regime, which occurs within the engine, is detected by the *NB_index* provided by the model: *NB_index<0* refers to forced convection flow regime, *0<NB_index<1* indicates that nucleate boiling flow regime occurs, while *NB_index>1* denotes the occurrence of the fully developed boiling (Fig. 2).

The controlled variable, which allows the achievement of the above control strategy, is the coolant flow rate. A proper correction is enforced to the coolant flow rate in order to obtain the desired *NB_index* value. The operating principle of the model-based control strategy is summarized in Figure 3. While the engine is running, the model receives the input variables (*rpm, p_{in}*,..) in real time and computes spatial-averaged engine wall and coolant temperatures as well as the *NB_index*.

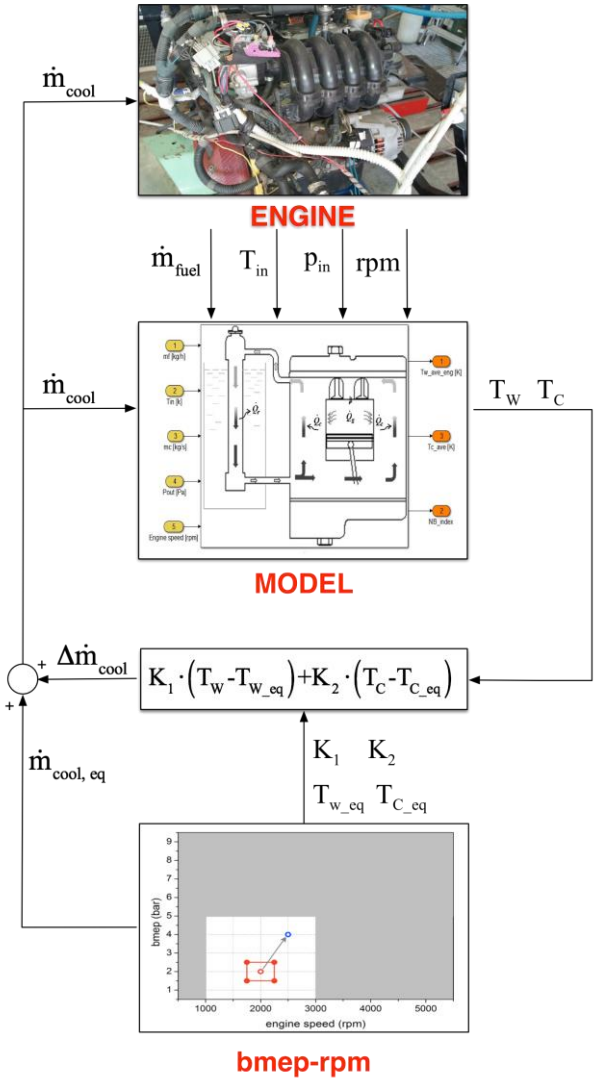

Fig.3 Engine control strategy

The controller values, K_1 and K_2, whose calculation procedure will be described in the following paragraph, are used in the following expression:

$$\Delta\dot{m}_c = K_1\left(T_w - T_{w\_eq}\right) + K_2\left(T_c - T_{c\_eq}\right) \qquad (7)$$

Eq. (7) estimates the value of $\Delta\dot{m}_c$, which is the correction to be given to the equilibrium coolant flow rate in order to satisfy the problem constraints on the desired values of T_{w_eq} and T_{c_eq}.

These variables are strictly related to the *NB_index*: in the proposed strategy, the desired equilibrium engine wall and coolant temperatures, are, in fact, selected in order to provide forced convection flow or light nucleate boiling regime at engine cold start and more developed nucleate boiling at fully warmed conditions. T_w and T_c are the actual engine wall and coolant temperatures. The values of the controllers K_1 and K_2 are estimated following the approach presented in Kothare et al. [18] and details can be found in the following paragraph.

3.1 Problem formulation

For the control system design, the mathematical model of the cooling system, which is described through eq. (1) and (2), can be expressed in the form of a discrete-time linear state-space system:

$$x(k+1) = A(k)x(k) + B(k)u(k) \quad (8)$$

$$y(k) = C(k)x(k) + D(k)u(k) \quad (9)$$

where k is the time in the discrete-time domain, $x = [T_w \;\; T_c]^T$ is the state of the system, $u = \left[\dot{m}_f \;\; \dot{m}_c \; T_{in} \;\; p_{out} \; N\right]^T$ is the vector of system inputs and $y = [T_w \;\; T_c \;\; NB\_index]^T$ is the system output. $[A(k)\; B(k)] \in \Omega$ and $\Omega = Co\{[A_1\; B_1], [A_2\; B_2], \ldots\ldots [A_n\; B_n]\}$ is the convex hull of matrices A_j, B_j, j =1,…, n. These matrices define the vertices of the polytopic domain, which includes all the possible evolutions of the non-linear system. C links the output variables to the state of the system and D correlates the output variables to the input ones. In our case, the only input variable, which can be actually manipulated, is the coolant flow rate $u_2 = \dot{m}_c$; the other input quantities are considered as noises.

The robust static state-feedback control problem of determining the coolant flow rate, which is necessary to obtain the desired output (*NB_index*) from the discrete-time system, can be formulated as:

$$u_2(k) = K * x(k) \quad (10)$$

The matrix K is the state-feedback control law, which minimizes the quadratic cost function:

$$J\left(k\right)=\sum_{i=0}^{p}\left[x\left(k+i\right)^{T}*Q_{1}*x\left(k+i\right)+u\left(k+i\right)^{T}*R*u\left(k+i\right)\right] \quad (11)$$

where p is time horizon and i is the time index; Q_1 and R are symmetric weighting matrices; in our case p=1. The state-feedback control matrix K is given by:

$$K=Y*Q^{-1} \quad (12)$$

Q and Y are obtained from the solution of the following linear objective minimization problem [18]:

$$\min_{g,Q,Y} \; g \quad (13)$$

where γ is the worst case (largest) value of the objective function *J(k);* the minimization problem is subject to the constraints on the system outputs and inputs and on system stability, which are expressed in form of Linear Matrix Inequalities (LMI):

$$\begin{bmatrix} 1 & x(k)^{T} \\ x(k) & Q \end{bmatrix} \geq 0 \quad (14)$$

$$\begin{bmatrix} Q & Q*A(k+i)^{T}+Y^{T}*B(k+i)^{T} & Q*Q^{\frac{1}{2}} & Y^{T}*R^{\frac{1}{2}} \\ A(k+i)*Q+B(k+i)*Y & Q & 0 & 0 \\ Q^{\frac{1}{2}}*Q & 0 & \gamma*I & 0 \\ R^{\frac{1}{2}}*Y & 0 & 0 & \gamma*I \end{bmatrix} \geq 0 \quad (15)$$

$$\begin{bmatrix} {u_{max}}^{2}I & Y \\ Y^{T} & Q \end{bmatrix} \geq 0 \quad (16)$$

$$\begin{bmatrix} Q & [A(k+i)*Q+B(k+i)*Y]^T*C^T \\ [A(k+i)*Q+B(k+i)*Y]*C & {y_{max}}^2*I \end{bmatrix} \geq 0 \qquad (17)$$

The controller was designed in order to satisfy the following specifications:

a. ensure the stability of the controlled system;
b. take into account the limitations of the actuators (i.e. maximum pump flow rate) and the maximum values of the input variables;
c. ensure the limitations of the output variables (i.e. wall and coolant temperatures) in order to guarantee engine reliability.

As the set of inequalities (14)-(17) may not have a solution if the range of the variables is to large, the fuel flow rate–speed range must be split into small sub-regions and the controllers (K_1, K_2) are to be calculated for each of them, in order to satisfy the restrictive specifications listed above. In addition, as the tendency to nucleate boiling and the *NB_index* are heavily influenced by the coolant pressure, *p*, (Fig. 2), for each sub-region two K matrices were calculated, one for p=0.5-1.5 bar and another for p=1.5-2.5 bar. When the engine operating condition varies within the full load and speed ranges, the controller switches to the (K_1, K_2) values of the sub-region which contains the new operating point (piecewise control approach). A typical engine speed-bmep sub-region is depicted in Fig.4.

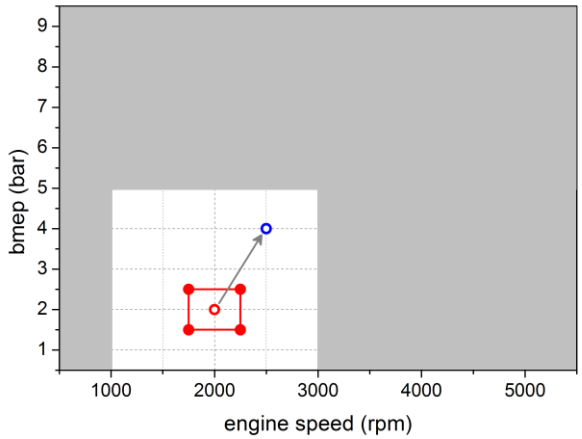

Fig.4 Engine map split in sub-regions for implementation of piecewise control strategy.

3.2 Controller design procedure

For nonlinear systems with a large operating field it is convenient to split it into small sub-regions (Fig. 4) and, with an off-line procedure, to design for each of them a specific predictive controller with estimate of its range of stability; this range must be large enough to cover also part of the adjacent sub-regions. The single controllers are then used during the actual on-line operation of the physical system by switching from one controller to another according to the operating condition. This achieves smooth transitions among the different operating sub-regions with guaranteed stability [23]. In the reported specific case the usual torque-engine speed plane was split into small fuel flow rate – engine speed sub-regions and for each of them the following steps are taken.

3.2.1 The nonlinear system described by the eq. (1) and (2) is linearized in the vertices of the considered sub-region (Fig. 4) and a set of matrices *A, B, C, D,* (eq. 8 and 9) is obtained for each vertex.

3.2.2. The constraints for the input (expected maximum and minimum engine-in coolant temperature, pressure and flow rate, fuel flow rate and engine speed) and output (allowed maximum and minimum values of average coolant temperature, wall temperature and *NB_index*) quantities are defined.

3.2.3. The minimization defined by eq. (13) with the inequalities (14)-(17) is then performed; the matrices *Y* and *Q* (eq. 12) are obtained and the controller $K = YQ^{-1}$ is computed. If the selected constraints are too tight (range of the input variables too wide and/or allowed range of the output variables too small), the minimization problem may not have a solution or the ellipsoids which guarantee stability [23] may be too small. In these cases, the size of the sub-regions used for the linearization must be reduced and/or the constraints must be relaxed. The process described by points 3.2.1 and 3.2.2 must then be repeated. If there is a solution to the min-max problem and it is satisfactory, a situation like the one depicted in Figure 5 will be obtained. The ellipsoid 1 in Figure 5 refers to the cold engine operation (coolant temperature less than 80 °C); the ellipsoid is large enough, to cover the entire fuel flow rate-engine speed range. In the case of fully warmed condition, the ellipsoids, which define the stability region for each of the fuel flow rate – engine speed sub-region overlap for more than ¾ of their area, thus enabling smooth transitions from

one sub-region to another with guaranteed stability during the actual on-line control. In addition to the defined sub-region, the above described process must be repeated for two different ranges of the coolant pressure: p=0.5-1.5 bar and p=1.5-2.5 bar.

3.2.4 A simulation software, which incorporates both the engine model [12] and the controller, is then used for a first check of the controller performance. During these on-line simulations, the controller selects the proper K_1, K_2, $T_{w\text{-}eq}$, T_{c_eq} values from multi-dimensional look-up tables on the basis of the fuel flow rate, engine speed and coolant pressure values. The on-line controller definition is, therefore, rapid and error-free.

3.2.5 The controller is then executed at the engine test rig for the final validation. Here a data acquisition system transfers the engine variable values to the model at a rate of 1.07 samples/s; the controller computes the coolant flow rate correction and enforces the proper voltage to the coolant electric pump at a rate of 1.02 samples/s in order to satisfy the thermal management strategy specifications (Fig. 6).

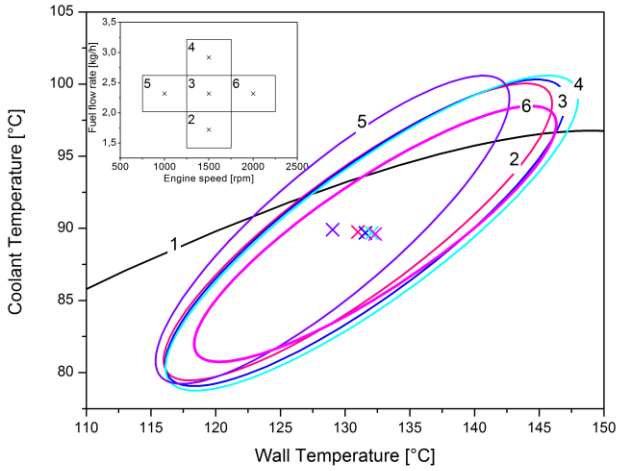

Fig.5 Ellipsoids that define the controller stability region for each of the fuel flow rate - engine speed sub-regions depicted in the upper-left corner.

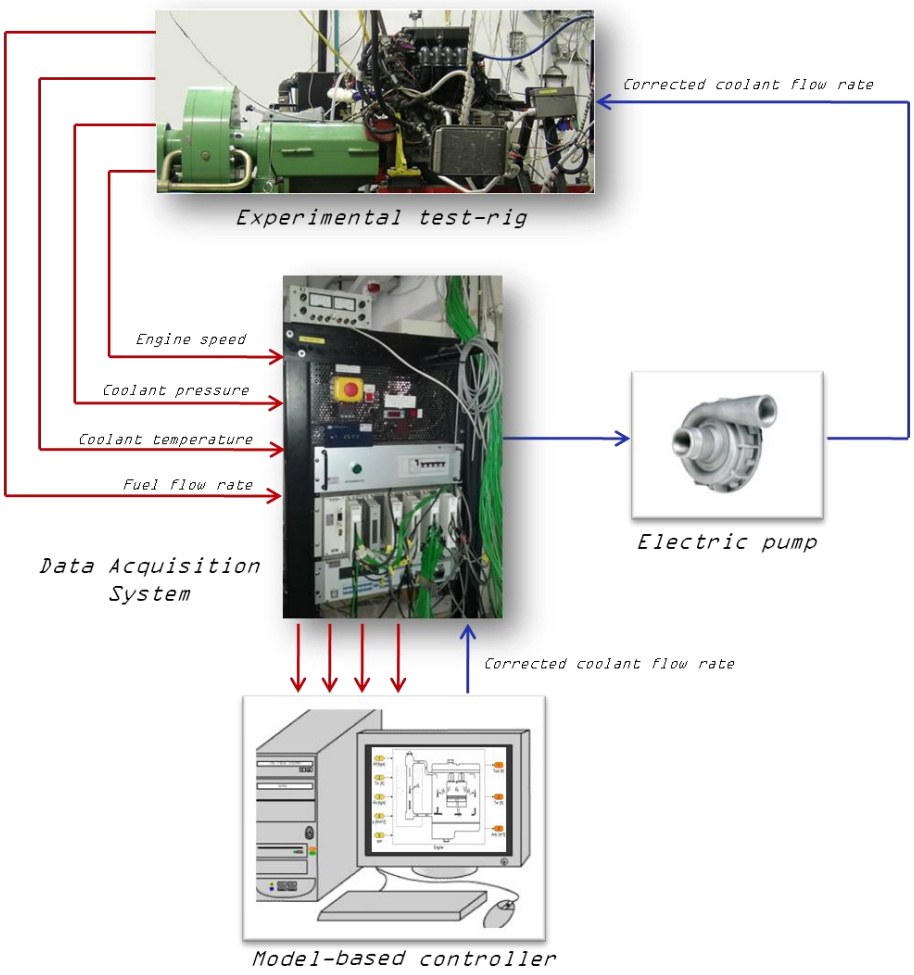

Fig.6 Schematic of the integration between the engine test rig and the controller.

4. EXPERIMENTAL TESTS

4.1 Experimental set-up

The test bench used for the experimental campaign is shown in Fig.7. The small four-stroke spark ignition engine displaces about 1.2 dm^3 in four in-line cylinders with four valves per cylinder and develops about 60 kW between 5000 and 6000 rpm. The standard crankshaft-driven coolant pump is substituted by a small power electric pump (127 W at 15 V, 2092 dm^3/h maximum flow rate). The test rig is equipped with a Borghi&Saveri FE 260-S eddy current

engine torque dynamometer provided with an actuator for remote control of throttle position and with an AVL 733S metering system for engine fuel consumption measurements. The coolant pressures at engine inlet and outlet are measured with miniature piezoresistive pressure transducers. PT100-type temperature sensors are used to obtain the coolant temperatures at engine inlet and outlet. Coolant volume flow rate is measured using turbine type flowmeters, with a repeatability of ±0.05%. K-type thermocouples are located in the cylinder block (head gasket side) and in the cylinder head at various locations. The standard radiator is air cooled for the warm-up tests, while it is immersed in a tank filled with water for the fully warmed tests, in order to keep the engine-inlet coolant temperature constant, at 85±1 °C. All tests are performed with a 50/50 (% by mass) mixture of water and commercially available ethylene glycol. Day-by-day repeatability was widely assessed and the results are reported in [12].

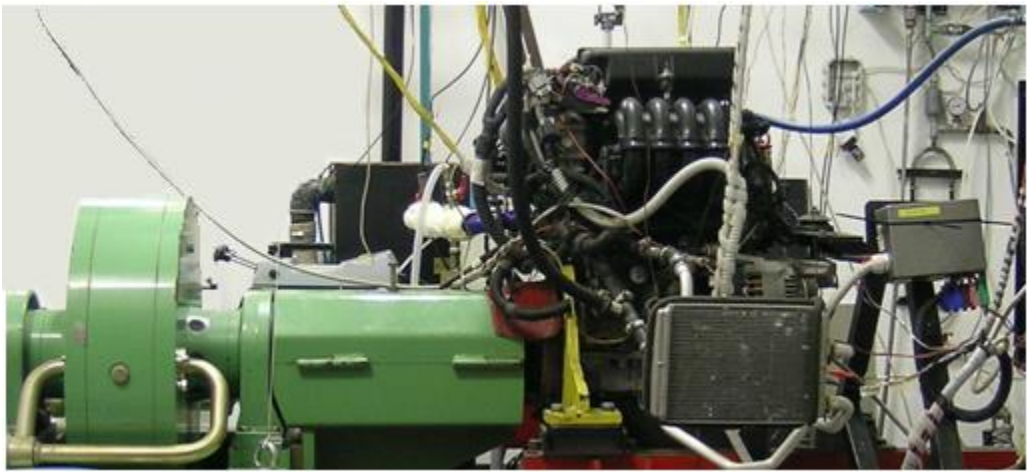

Fig.7 Engine test-rig.

4.2 Experimental activity

The experimental campaign was planned with the purpose of validating the control algorithm both during the warm-up and in transient conditions with the fully warmed engine. As for the fully-warmed conditions, initially, operating conditions within a single sub-region centered around *2000rpm* and *2bar* bmep (*2000x2*) were selected, where one single couple of K_1,

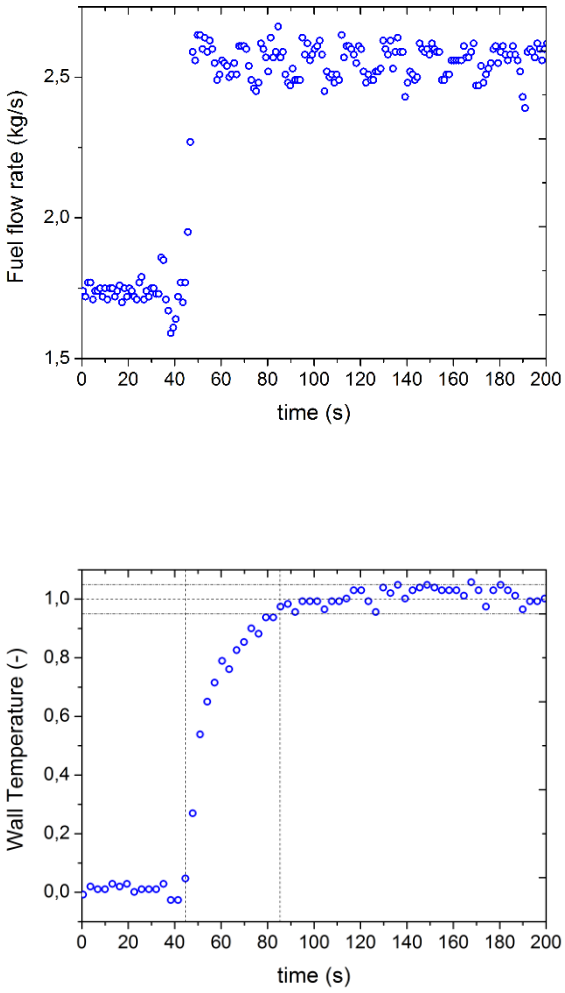

Fig.8 Engine typical response time: fuel flow rate (top) and wall temperature (bottom).

K_2 values of the controller is needed. Subsequently, step variations in engine speed and bmep were enforced, with operating conditions which involve a different sub-region and therefore the need to switch from one couple of K_1, K_2 values to another.

It is worth pointing out that the data acquisition rate is 1.07 s and the update rate of the controlling signal (pump voltage) is 1.02 s. Both rates are much shorter than the typical response time of the engine. In a modern fuel injection engine, the fuel flow rate is updated very fast, with a delay of the order of the engine cycle duration, in response to a request of torque variation. In the laboratory tests reported, this delay is of the order of 3 s for a step variation of the bmep from

2 to 4 bar (Fig. 8, top). As a result of this input variation, the wall temperature adaptation is much slower with a settling time of about 40 s (Fig.8, bottom). The settling time of the coolant temperature is very similar, about 35s. The update rate of the control signal is therefore adequate.

5. RESULTS

The following sections summarize the results of an experimental campaign carried out with the aim to test the control algorithm both during engine warm-up and under fully warmed conditions. The engine operating condition is fixed at 2000 *rpm* x 2 *bar* bmep and the cold start initial temperature is about 25°C both for coolant and engine metal.

5.1 Engine warm-up control strategy

The purpose of the cold start control strategy is the reduction of the engine warm-up time. In this case, the radiator was air-cooled, the thermostatic valve was removed and the engine operating conditions were fixed to 2000 rpm x 2 bar bmep; the tests have, therefore, the aim to illustrate the behavior of the controller, rather than to make comparison with a conventional cooling system during real warm-up. The operating conditions were selected in order to have a single couple of K_1, K_2 values for the warm-up; in addition, the values of K_1, K_2 were obtained by requiring single phase forced convection ($-1<NB\_index<0$).

Figure 9 shows the coolant flow rate, the wall and coolant temperatures and the coolant flow rate corrections enforced by the controller as a function of time. In Fig. 9 (top), the dashed curve represents the coolant flow rate that would be supplied by a mechanical pump at this engine speed; its value is approximately 2000 dm^3/h. The value of coolant flow rate is strongly reduced when the controller is enabled. The result obtained with three different values of the equilibrium (desired) wall temperature are presented (T_{w_eq}=65°C, 90°C and 110°C). For each of the above equilibrium wall temperature values, the coolant flow rate at cold start is very low; it then increases rapidly as the engine wall temperature increases (Fig. 9 middle). After this first stage, the coolant flow rate remains rather constant or increases slightly as a result of two opposite corrections that the controller imposes (Fig. 9, bottom). The first one is due to the wall temperature, which is significantly lower than the equilibrium (desired) one T_{w_eq}; in this case, the controller enforces a reduction of the coolant flow rate ($K_1>0$) with respect to the equilibrium value (~1050 dm^3/h). A lower coolant flow rate, in fact, facilitates the wall temperature increase.

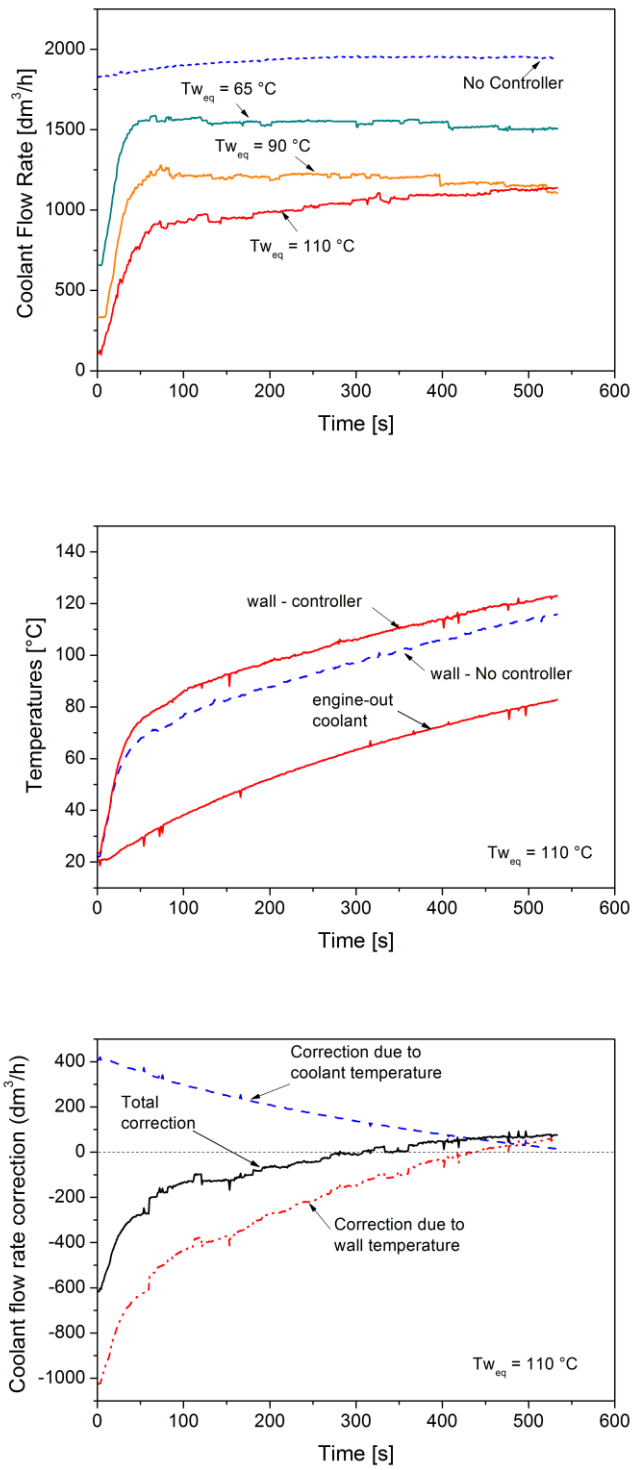

Fig.9 Coolant flow rate during the engine warm-up with and without controller (top); corresponding engine wall temperature evolution (middle); contributions to the coolant flow rate correction (bottom).

The second correction is due to the coolant temperature, which is also lower than the desired value. In this case, on the contrary, the correction is toward an increase of the coolant flow rate (K_2<0). In fact, an increase of the coolant flow rate facilitates the coolant temperature increase. The correction, which is due to the wall temperature, is stronger, so that the total effect is a reduction of the coolant flow rate with respect to its equilibrium value. These corrections, however, diminish rapidly as the wall and coolant temperature approach their equilibrium values. As a result, the coolant flow rate varies slowly after the first 100 s. The fastest warm-up was obtained for T_{w_eq}=110°C. Therefore, in the following discussion only the results with T_{w_eq}=110 °C will be presented; they will focus on the warm-up duration which ends when the coolant temperature reaches the equilibrium value of 85°C. In Fig. 9 (middle), as expected, the engine wall temperatures, obtained when the controller is enabled, are higher. In addition, the wall temperature increases much more rapidly than the coolant temperature in the first 50 s; after that, their rate of change is similar.

When the control is active, the faster temperature increase, which can be observed close to the inlet valves, shortly after engine start, has important effects on the engine performances. Figure 10 shows the air fuel ratio as a function of time both with and without controller. In the early 120 s the A/F ratio obtained when the control is active is higher owing to the higher wall temperatures which promote a faster fuel evaporation and consequently a better air fuel mixing; this contributes to reduce the specific fuel consumption and, presumably, the fraction of unburned HC at the exhaust (not monitored in this work). A further advantage deriving from higher engine wall temperatures, which allows a reduction in fuel consumption, is the faster heating of the lubricant (Fig. 11). The lower lubricant viscosity reduces the mechanical power needed by the lubricant pump, and also contributes to reduce the frictional losses within the engine mechanical components.

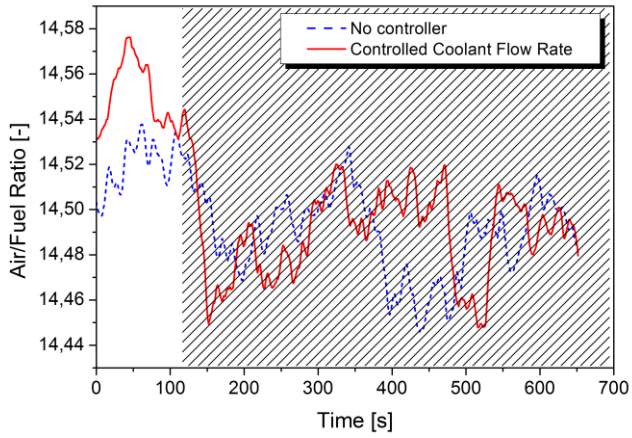

Fig.10 Measured air-fuel ratio with and without controller (top).

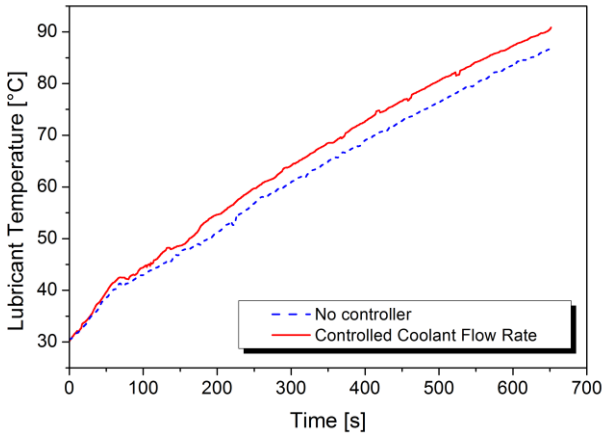

Fig.11 Lubricant temperature measured both with and without controller.

The fuel consumption reduction obtained by the introduction of the control strategy is displayed in Fig.12. The reduction in fuel consumption over the warm up time is found in the range 1-3%, taking into account the day-by-day variation.

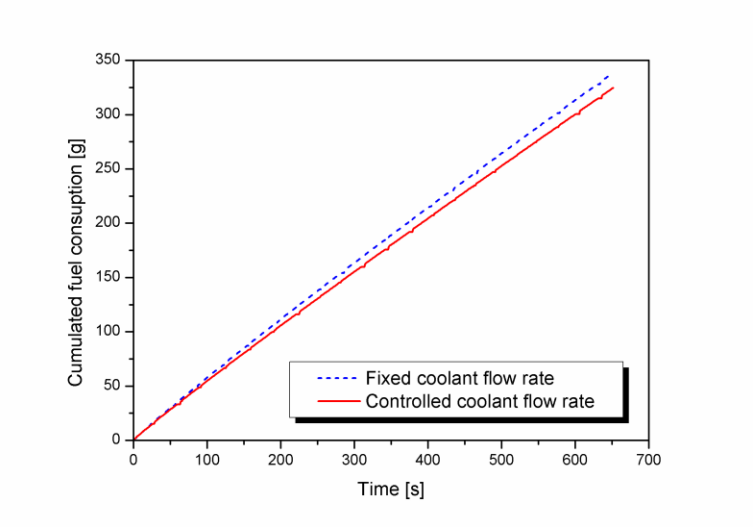

Fig.12 Fuel consumption during the engine warm-up.

5.2 Fully warmed control strategy

Under fully warmed operating conditions, the purpose of the control strategy is to keep the engine working under nucleate or saturated boiling conditions. As a consequence, the controller will act on the electric pump in order to enforce the proper value of coolant flow rate, which determines nucleate or saturated boiling flow regime.

The first experimental test was carried out by starting the engine and enforcing the operating condition 2000*rpm* x 2 *bar* bmep. In these tests, the radiator was immersed in tank filled with water and engine-in coolant temperature was kept at 85±1 °C. The controller was tested within a region of the *rpm- bmep* plane small enough in order to allow the use of a single couple of values K_1, K_2 (eq. 7, fig. 4). Different operating conditions were enforced according to the path displayed in Fig. 13 (top)**.**

Fig. 13 (bottom) shows the *NB_index* vs. *time* for each operating point. It can be observed, that the *NB_index* values are within the range 0-1 for most of the operating conditions (points 1-3, fig.13 a), indicating thus that nucleate boiling flow regime is achieved. On the contrary, at *1500x3* (point 4) and *1500x1* (point 5), the *NB_index* value is negative and the forced convention

flow regime occurs. The controller, therefore, fails in this sub-domain, and consequently, a reduction of the control area was operated Fig. 14 (top).

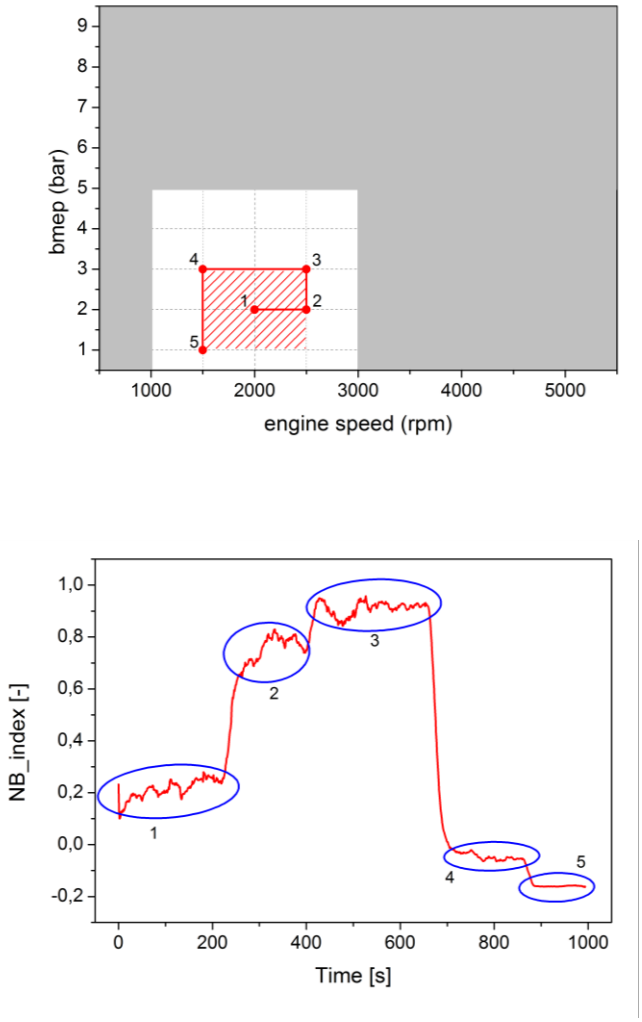

Fig. 13 Engine operating conditions enforced (top) for a single couple of (K_1, K_2) controller values; resulting *NB_index* (bottom). The constraints on *NB_index* are not completely satisfied.

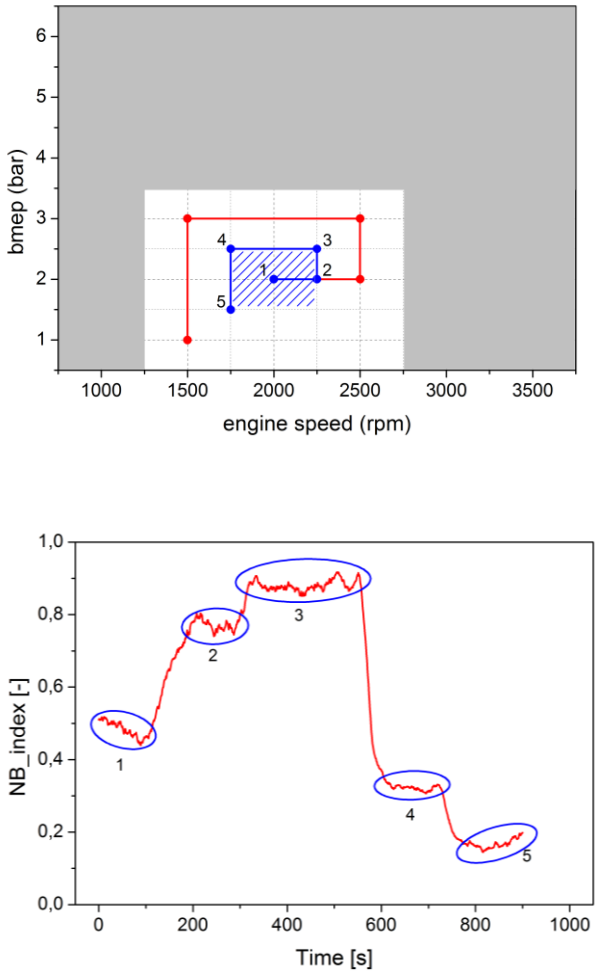

Fig. 14 Engine operating conditions enforced in a reduced sub-region (blue, top) for a single couple of (K_1, K_2) controller values ; resulting *NB_index* (bottom). The constraints on *NB_index* are completely satisfied.

In this case, the *NB_index* value stays in the desired range for each operating point Fig. 14 (bottom). Figure 15 shows the coolant flow rate set by the controller and the actual flow rate measured at the engine inlet; minor differences can be observed, which are due to nonperfect calibration of the pump voltage-flow rate characteristic at the different coolant temperatures.

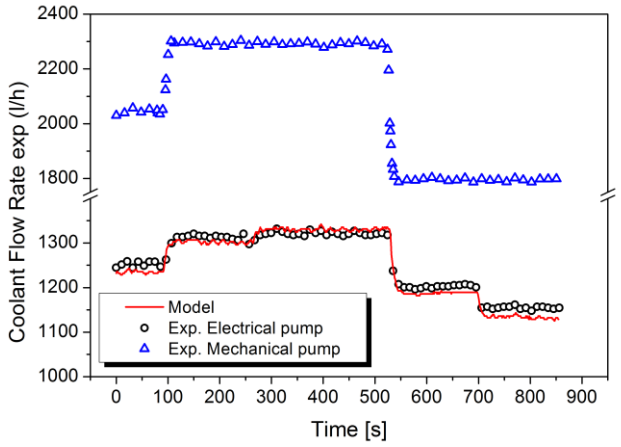

Fig.15 Experimental coolant flow rate obtained with the mechanical pump and with the control (symbols) and comparison with the flow rate calculated by the model (line).

Figure 16 presents the record of a further experimental test, which was carried out by enforcing a set of different operating conditions in terms of fuel flow rate and engine speed. The tests involve both bmep variations at constant engine speed and engine speed variation at constant bmep. In these conditions, the controller will use different couples of (K_1, K_2) values. The results of the controller action are presented in figure 17. The coolant flow rate seems to follow the trend of the fuel flow rate; the reason for this is actually because the variations of fuel flow rate are much more significant (ratio 5:1) than the ones of the engine speed (ratio 1:0.75). The *NB_index* remains within the 0-1 range, which was specified as a constraint for the control design, thus allowing a moderate nucleate boiling.

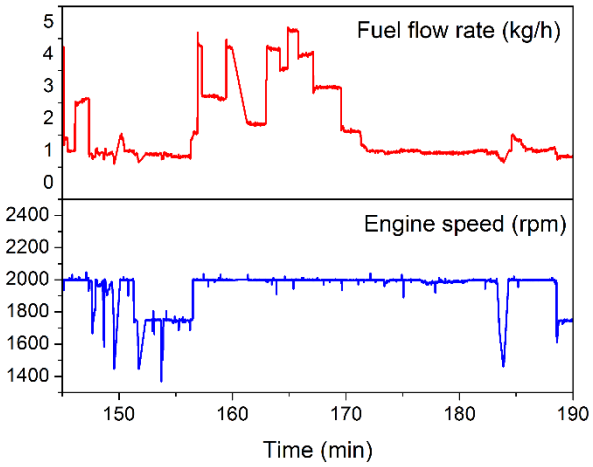

Fig.16 Operating conditions covering different sub-regions: Fuel flow rate (top) and engine speed (bottom).

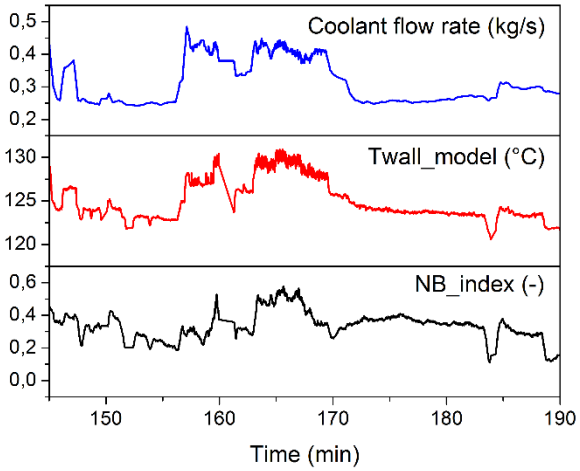

Fig.17 Experimental coolant flow rate (top), model predicted average engine wall (middle) and model predicted *NB_index* (bottom) as a result of the operating conditions of fig.16.

In Figure 18 a more detailed view around the time 164 min is presented. In this region a step variation of the bmep and therefore of the fuel flow rate is enforced at constant engine speed. As a result of the control action, the coolant flow rate increases and so does the average

wall temperature predicted by the model. Also the *NB_index* increases, which however, still remains within the 0-1 interval (Fig. 19).

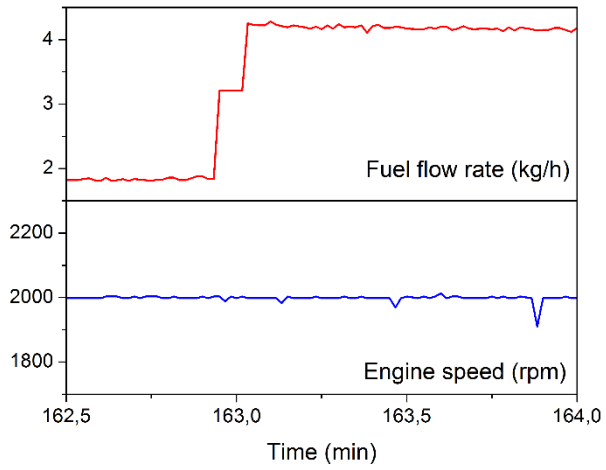

Fig.18 Engine operating conditions: bmep step at constant engine speed. Fuel flow rate (top), engine speed (bottom).

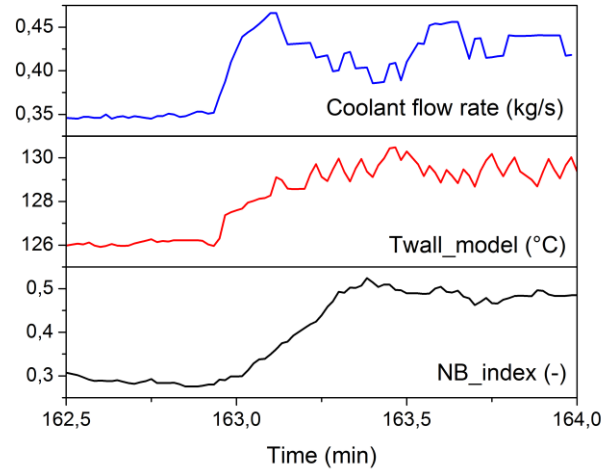

Fig.19 Experimental coolant flow rate (top), model predicted average engine wall (middle) and model predicted *NB_index* (bottom) as a result of the operating conditions of fig.18.

Finally, Figure 20 shows the case of engine speed decreasing at constant bmep; here, the fuel used per engine cycle remains constant, but the fuel flow rate diminishes proportional with the engine speed. As a result, both coolant flow rate and wall temperature diminish (Fig. 21).

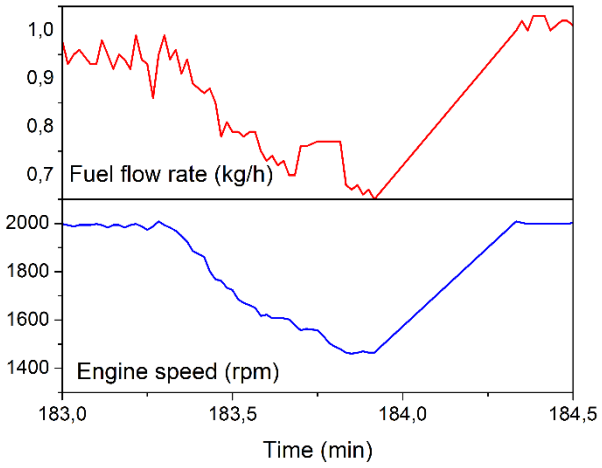

Fig.20 Engine operating conditions: constant bmep and variable engine speed. Fuel flow rate (top), engine speed (bottom).

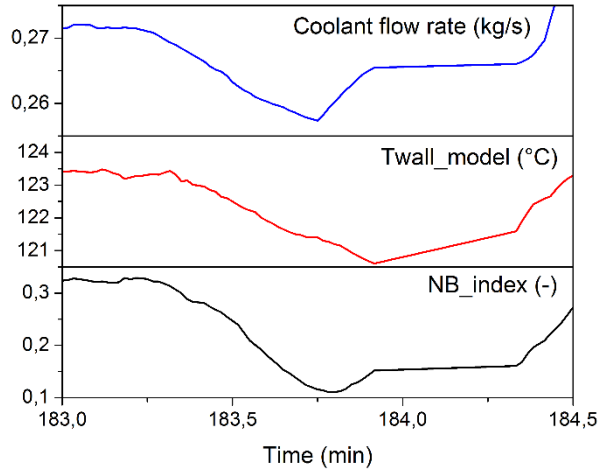

Fig.21 Experimental coolant flow rate (top), model predicted average engine wall (middle) and model predicted *NB_index* (bottom) as a result of the operating conditions of fig.20.

6. SUMMARY AND CONCLUSIONS

A Model Predictive Control was successfully set up to manage the coolant flow rate in the cooling system of an internal combustion engine. The scheme makes use of a zero-dimensional model [12] to obtain the value of variables, which are not usually available on board a vehicle, such as the metal temperature, or others that cannot be measured on a real engine, like the distance of the heat transfer regime from the onset of nucleate boiling.

The model [12] is first used off-line to obtain a couple of values (K_1, K_2), which define the controller. These values are obtained through the robust methodology proposed by Kothare et al. [18,23]. Once these values for (K_1, K_2) are known, the model is used on-line to predict the values of the average coolant temperature and average metal temperature (state variables of the model). On the basis of these temperatures and of the previously computed (K_1, K_2) the coolant flow rate is determined and imposed by means of an electric pump.

Two general thermal conditions were considered: engine warm-up and fully warmed engine. In the first case, a single couple of values (K_1, K_2) is enough for the controller. In the case of fully warmed engine, on the contrary, the engine speed–fuel flow rate plane must be divided into sub-regions (piece-wise control) and, as the constraints become narrower, the number of these sub-regions and the number of (K_1, K_2) couples of values increase. A number of 50-100 sub-regions is typically necessary.

The controller was validated at the engine test rig and proved to be robust in terms of disturbance rejections and respect of the constraints and very fast in terms of response to the perturbations. The experimental tests provided that the proposed control is effective in decreasing the warm-up time and in reducing the coolant flow rate under fully warmed conditions as compared to a standard configuration with pump speed proportional to engine speed.

In the proposed application the distance of the thermal heat regime from the onset of nucleate boiling was selected as a constraint. The model is, however, very flexible and other constraints and objective functions can be adopted, also in the perspective of the future homologation cycles, which are currently being considered by the regulatory Agencies.

More work, however, is needed to make the comparison meaningful in terms of NEDC performances.

7. ACKNOWLEDGEMENTS

The investigation was funded by the Italian Ministry of University and Research under the project PON01_01517, CUP: B21H11000400005, with financial support of the European Commission. The precious suggestions of prof. Giuseppe FRANZÉ for the design of the control algorithm and the help of the PhD student Walter LUCIA for implementing the needed computer code is gratefully acknowledged.

REFERENCES

1. Regulation (EC) No 715/2007
2. EC. Setting emission performance standards for new passenger cars as part of the community's integrated approach to reduce CO_2 emissions from light-duty vehicles, No. 443/2009, Off J Eur Union, 2009.
3. Cipollone, R., Di Battista, D. Sliding vane rotary pump in engine cooling system for automotive sector. Appl Therm Eng. 2015; 76:157-166. DOI:10.1016/j.applthermaleng. 2014.11.001.
4. Roberts, A., Brooks, R., Shipway, P. Internal combustion engine cold-stat efficiency: A review of the problem, causes and potential solutions. Energ Convers Manage. 2014; 82:327-350. DOI:10.1016/j.enconman.2014.03.002.
5. Heywood, J.B. Improving the Spark-Ignition Engine. Capri, oral presentation ICE 2005; 7th International Conference on Engines for Automobile, Capri, September 11-16, 2005.
6. Will, F., Boretti, A. A new method to warm up lubricating oil to improve the fuel efficiency during cold start. SAE Int. J. Engines 2011; 4(1):175-187. DOI: 10.4271/2011-01-0318.
7. Trapy, J.D., Damiral, P. An investigation of lubricating system warm-up for the improvement of cold start efficiency and emissions of SI automotive engines. SAE technical paper 902089, 1990. DOI:10.4271/902089.
8. Will, F. Fuel conservation and emission reduction through novel waste heat recovery for internal combustion engines. Fuel 2012; 102:247–55. DOI:10.1016/j.fuel.2012.06.044.
9. Samhaber, C., Wimmer, A., Loibner, E. Modeling of engine warm-up with integration of vehicle and engine cycle simulation. SAE technical paper 2001-01-1697, 2001; 55-62.
10. Cheng, W.K., Hamrin, D., Heywood, J.B., Hochgreb, S., Min, K, and Norris, M. An Overview of Hydrocarbon Emissions Mechanisms in Spark-Ignition Engines. SAE paper

932708, presented at the SAE Fuels and Lubricants Meeting and Exposition, Philadelphia, PA, October 18-21, SAE Trans., Vol. 102, 1993.

11. Gardiner, R., Zhao, C., Addison, J., Shayler, P.J. The effects of thermal state changes on friction during the warm up of a spark ignition engine. Presented at VTMS 11, Coventry, UK; 2013.
12. Bova, S., Castiglione, T., Piccione, R., Pizzonia, F. A dynamic nucleate-boiling model for CO2 reduction in internal combustion engines. Appl Energ. 2015; 143:271-282. DOI:10.1016/j.apenergy.2015.01.047
13. Brace, C.J., Burnham-Slipper, H., Wijetunge, R.S., Vaughan, N.D., Wright, K., Blight, D. Integrated Cooling System for Passenger Vehicles. SAE Technical Paper 2001-01-1248, 2001. DOI: 10.4271/2001-01-1248.
14. Ap, N. and Golm, N. New Concept of Engine Cooling System (Newcool). SAE Technical Paper 971775, 1997. DOI:10.4271/971775.
15. Brace, C.J., Hawley, G., Akehurst, S., Piddock, M., Pegg, I. Cooling system improvements – assessing the effects on emissions and fuel economy. Proc Inst Mech Eng Part D: J Automob Eng 2008; 222(4):579–591. DOI: 10.1243/09544070JAUTO685.
16. Bent, E., Shayler, P., La Rocca, A. The effectiveness of stop–start and thermal management measures to improve fuel economy. Presented at VTMS 11, Coventry; 2013.
17. Barbarelli, S., Bova, S. and Piccione, R. "Zero-dimensional Model and Pressure Data Analysis of a Variable-Displacement Lubricating Vane Pump" , SAE paper n. 2009-01-1859, International Powertrains, Fuels & Lubricants Meeting June 15-17, 2009, Florence, Italy, 2009.
18. Kothare, M.V., Balakrishnan, V., Morari, M. Robust constrained model predictive control using linear matrix inequalities. Automatica 1996; 32(10):1361-1379. DOI:10.1016/0005-1098(96)00063-5.
19. Mayne, D.Q. Model predictive control: Recent developments and future promise. Automatica 2014; 50:2967–2986. DOI: 10.1016/j.automatica.2014.10.128.
20. Van Staden, A.J., Zhang, J., Xia, X. A model predictive control strategy for load shifting in a water pumping scheme with maximum demand charges. Appl Energ. 2011; 88(12): 4785–4794. DOI:10.1016/j.apenergy.2011.06.054.
21. Parisio, A., Rikos, E., Tzamalis, G., Glielmo, L. Use of model predictive control for experimental microgrid optimization. Appl Energ 2014; 115:37-46. DOI:10.1016/j.apenergy.2013.10.027.
22. Kwak, Y., Huh, J.H., Jang, C. Development of a model predictive control framework through real-time building energy management system data. Appl Energ. 2015; 155: 1–13. DOI:10.1016/j.apenergy.2015.05.096.

23. Wan, Z. and Kothare, M.,V., Efficient scheduled stabilizing model predictive control for constrained nonlinear systems, Int. J Robust Nonlinear Control, 2003; **13**:331-346 (DOI:10.1002/rnc.821).

24. Petersen, I.R., Tempo, R. Robust control of uncertain systems: Classical results and recent developments; Automatica 50 (2014) 1315–1335. DOI:10.1016/j.automatica.2014.02.042.

25. Amelio, M., Barbara, F., Bova, S., Oliva, P. Experimental Investigation on an ICE Cooling System under Nucleate Boiling Conditions. SAE Technical Paper 2001-01-1795, 2001. DOI: 10.4271/2001-01-1795.

26. Castiglione, T., Pizzonia, F., Piccione, R., Bova S., "Detecting the Onset of Nucleate Boiling in Internal Combustion Engines," Applied Energy 164:332-340, 2016, doi: 10.1016/ j.apenergy .2015.11.083.

27. Heywood, J.B., Internal Combustion Engine Fundamentals, McGraw-Hill, New York, 1988.

28. Dittus, F.W. and Boelter, L.M.K. Heat Transfer in Automobile Radiators of the Tubular Type. Univ. Calif. Publ. Eng. 1930; 2:443-461

29. Chen, J.C. Correlation for Boiling Heat Transfer to Saturated Fluids in Convective Flow. Ind. Eng. Chem. Process Des. Dev. 1966; 5(3):233-329. DOI: 10.1021/i260019a023.

FIGURES CAPTIONS

Fig.1 Model input and output variables

Fig.2 Predicted *NB_index* values for different coolant flow rates (top) and thermal power transferred to the coolant as a function of the volumetric coolant flow rate (bottom). Symbols refer to calculated quantities during test-rig experiments. (Operating conditions: 200 rpm, 2 bar bmep).

Fig.3 Engine control strategy.

Fig.4 Engine map split in sub-regions for implementation of piecewise control strategy.

Fig.5 Ellipsoids that define the controller stability region for each of the fuel flow rate - engine speed sub-regions depicted in the upper-left corner.

Fig.6 Schematic of the integration between the engine test rig and the controller.

Fig.7 Engine test-rig.

Fig.8 Engine typical response time: fuel flow rate (top) and wall temperature (bottom).

Fig.9 Coolant flow rate during the engine warm-up with and without controller (top); corresponding engine wall temperature evolution (middle); contributions to the coolant flow rate correction (bottom).

Fig.10 Measured air-fuel ratio with and without controller.

Fig.11 Lubricant temperature measured both with and without controller.

Fig.12 Fuel consumption during the engine warm-up.

Fig.13 Engine operating conditions enforced (top) for a single couple of (K_1, K_2) controller values ; resulting *NB_Index* (bottom). The constraints on *NB_index* are not completely satisfied.

Fig.14 Engine operating conditions enforced in a reduced sub-region (blue, top) for a single couple of (K_1, K_2) controller values ; resulting *NB_Index* (bottom). The constraints on *NB_index* are completely satisfied.

Fig.15 Experimental coolant flow rate obtained with the mechanical pump and with the control (symbols) and comparison with the flow rate calculated by the model (line).

Fig.16 Operating conditions covering different sub-regions: Fuel flow rate (top) and engine speed (bottom).

Fig.17 Experimental coolant flow rate (top), model predicted average engine wall (middle) and model predicted NB_index (bottom) as a result of the operating conditions of Fig. 16.

Fig.18 Engine operating conditions: bmep step at constant engine speed. Fuel flow rate (top), engine speed (bottom).

Fig.19 Experimental coolant flow rate (top), model predicted average engine wall (middle) and model predicted NB_index (bottom) as a result of the operating conditions of Fig. 18.

Fig.20 Engine operating conditions: constant bmep and variable engine speed. Fuel flow rate (top), engine speed (bottom).

Fig.21 Experimental coolant flow rate (top), model predicted average engine wall (middle) and model predicted NB_index (bottom) as a result of the operating conditions of Fig. 20.